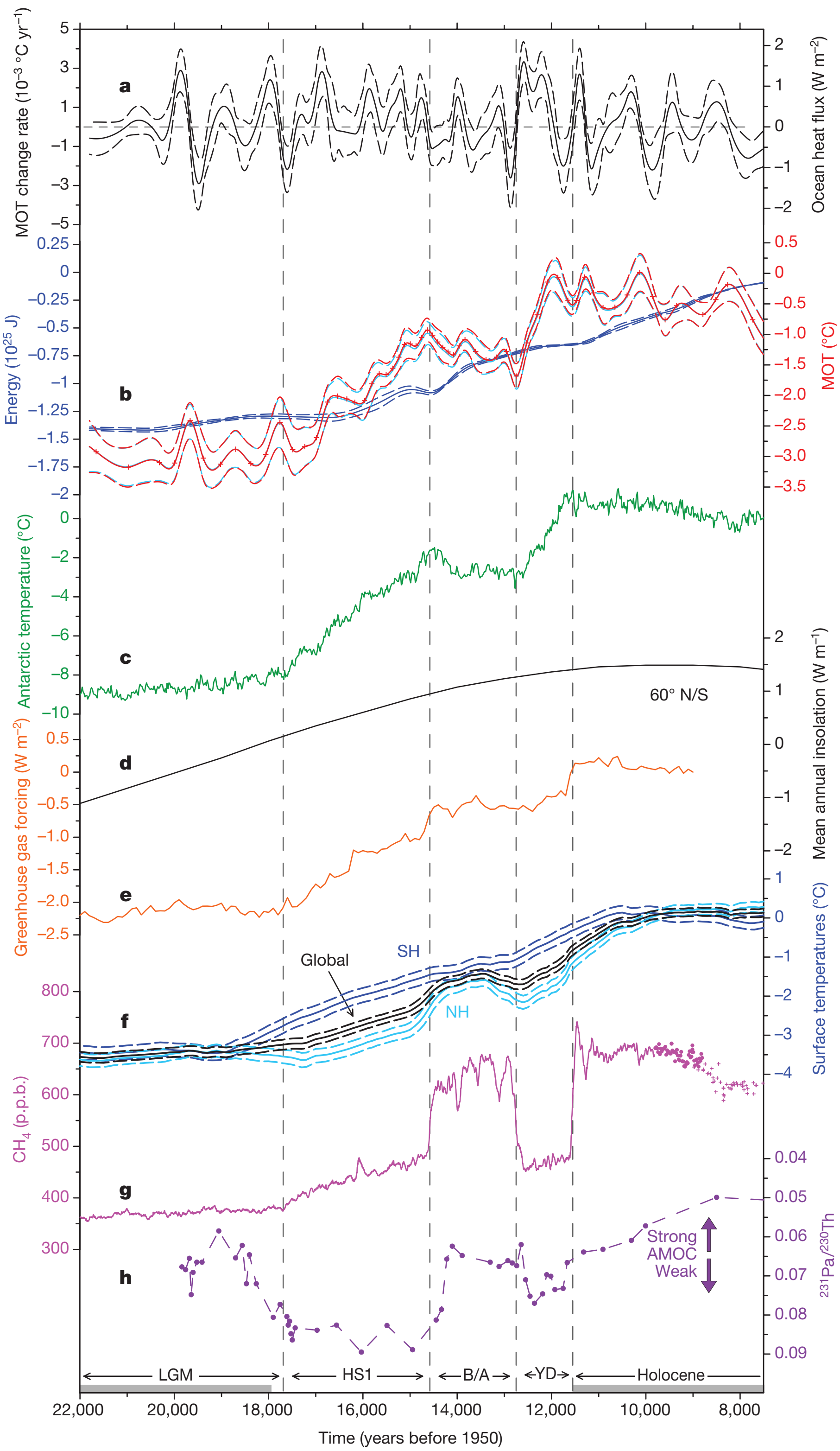

Figure 3 | Comparison of our best-estimate MOT record with other palaeoclimatic records for the last glacial transition. Labels as in Fig. 2. The grey bars mark the sections used to derive the LGM–Holocene MOT difference. **a**, MOT change rate and corresponding global ocean heat flux derived from Monte Carlo splining of our best-estimate MOT dataset with 600-yr cut-off frequency splines. The uncertainty band (dashed lines) represents the 1σ range of all realized Monte Carlo splines. **b**, The red lines are the splined version of our best-estimate MOT dataset (Fig. 2, red) using the same splining procedure as in **a**. Note that caution is required when interpreting excursions based on single data points, such as for example, around 20 kyr BP (also applies to **a**). The light-blue lines are the energy anomaly in the total ocean relative to today expressed in the same type of spline as for the red curve. The left y axis is scaled such that the light-blue and red curves overlap as much as possible. The remaining small difference originates from the different effect of ocean volume change on the two parameters. Crosses indicate where the actual data points are located. The dark-blue lines are the sea-level anomaly record of ref. 14 transferred into the latent energy put into melting (grounded) ice to create the corresponding sea-level change (the LGM low corresponds to a sea level 134 m below today's). The splining procedure is the same as above, but with a cut-off frequency of 150 yr (because of the higher resolution of this record) and a 2σ uncertainty band. The latent heat is derived by simple scaling of the sea-level data by $3.45 \times 10^{14}\,m^3$ ocean volume change per metre of sea level[14] and the latent heat coefficient for the ice–water transition (thermal expansion contribution (about 0.6 m between the LGM and the Holocene) can be neglected). **c**, Antarctic temperature reconstruction[39]. **d**, 60° N and 60° S (roughly where deep waters are formed) mean annual insolation anomaly relative to today[40], which is driven by changes in obliquity and is symmetric on both hemispheres. **e**, Greenhouse gas forcing[41]. **f**, Reconstructed Earth surface temperatures with 1σ uncertainty band of Northern Hemisphere ('NH', light blue), Southern Hemisphere ('SH', dark blue), and global average ('Global', black)[6]. **g**, Atmospheric CH_4 measured at the WAIS divide ice core[29]. **h**, AMOC proxy $^{231}Pa/^{230}Th$ from ocean sediment core OCE326-GGC5 recalibrated with IntCal13[30,42]. All data are plotted on their original age scale if not otherwise noted (WD2014 for WAIS data[36]). Note that the data shown in **b**–**f** are anomalies relative to today.

seven different global climate models (six are part of the Paleoclimate Modelling Intercomparison Project 3 (PMIP3)) that provided such output for LGM and preindustrial conditions (see Methods). All these independent state-of-the-art climate models have different but physically consistent climatologies for the two climate states, for which reason the model ensemble spread is representative of the uncertainties of how MOT, ASST and GAST are linked. The model ensemble ranges of the scaling factor for ΔASST/ΔMOT and ΔGAST/ΔMOT are 0.7–0.9 and 2.0–2.9, respectively. The models generally underestimate the LGM–Holocene MOT difference (range 0.9 °C to 2 °C) relative to our results. Despite the uncertainties related to these scaling factors, they suggest that the LGM–Holocene GAST difference is between 5.1 °C and 7.5 °C, which is roughly consistent with the estimates of refs 8 and 19, but not with the low values of ref. 6 and in particular of ref. 26. Note that most of these studies use PMIP climatologies to infer GAST as we do here, however, they use surface temperature proxies that are recording local climate and are affected by ocean biogeochemistry. Owing to the globally integrative and purely physics-driven nature of the MOT proxy